

Source scaling of intermediate-depth Vrancea earthquakes

A. Gusev,¹ M. Radulian,² M. Rizescu² and G. F. Panza³

¹*Institute of Volcanic Geology & Geochemistry, 9 Piip Blvd, 683006 Petropavlovsk-Kamchatskii, Russia*

²*National Institute for Earth Physics, PO Box MG-2, 76900 Bucharest, Romania. E-mail: mircea@infp.ro*

³*University of Trieste, Department of Earth Sciences, via Weiss 4, 34127 Trieste, Italy*

Accepted 2002 July 8. Received 2002 July 8; in original form 2001 October 16

SUMMARY

Source scaling properties are studied for the intermediate-depth seismic nest in the Vrancea region, Romania, which has been the source of many destructive earthquakes. We investigate spectral and time-domain scaling properties using wide-band digital records from 16 earthquakes ($3.7 \leq M_W \leq 7.4$). All processing variants (P or S waves, spectral or time domain, etc.) produce consistent results. The observed corner-frequency versus M_W trend generally follows the constant-stress-drop model, with typical stress-drop values of 1–10 MPa. This kind of scaling, seen over the entire magnitude range analysed, is similar to that observed for shallow events. However, this trend seems to be violated for the largest earthquakes ($M_W > 6.5$). They show a clear tendency for higher static stress drops than shallow events, and for magnitudes above 7, average stress drops exceeding 10 MPa may be expected. These results are of particular significance for seismic hazard studies, and specifically for the estimation of future strong motions.

Key words: source parameters, source scaling, Vrancea earthquakes.

INTRODUCTION

The Vrancea zone, located in Romania, at the sharp bend of the southeastern Carpathians (Fig. 1), is a well-defined seismic region in Europe with unique properties. The seismicity is concentrated in a confined, high-velocity, focal volume in the depth range 60–200 km. A relatively high seismic energy is persistently released (four shocks with magnitude greater than 7 during the past century) by a seismogenic process that is still far from being fully understood. At shallower levels (0–60 km), the seismicity is sporadic and weak (magnitude below 5.5), and seems to be decoupled from the seismic activity in the subcrustal lithospheric slab. The major intermediate shocks exhibit a quite stable reverse faulting focal mechanism with the rupture plane oriented in a NE–SW direction, parallel to the Carpathians arc.

Previous studies of the most recent strong intermediate-depth earthquakes (1940 November 10, $M_w = 7.7$; 1977 March 4, $M_w = 7.4$; 1986 August 30, $M_w = 7.1$; 1990 May 30, $M_w = 6.9$) based on teleseismic data have indicated static stress drop values around 10 MPa, and source durations in the range 3–10 s (for example, Räckers & Müller 1987; Monfret *et al.* 1990; Tavera 1991). Similar values of stress drop were obtained from the aftershocks: 5.0 MPa for the 1986 shock (Trifu & Oncescu 1987) and 11 MPa for the 1990 shock (Trifu *et al.* 1992). Enescu *et al.* (1979) computed a stress drop of 13.3 MPa for the 1940 Vrancea strong earthquake. Oncescu (1989) showed that the effective stress acting in the focal region of the 1986 shock is an order of magnitude higher than the static stress drop. He found that this $M_w = 7.1$ event was rich in high-frequency energy, corresponding in this respect to a typical event of surface wave magnitude $M_S = 7.9$. This may explain why very high accelerations were recorded at large hypocentral distances, even on hard rock.

The seismic source analysis performed for moderate Vrancea earthquakes ($M_w \sim 5$) suggested generally normal stress drop values as compared with shallow earthquakes of similar magnitude (Oncescu 1986; Radulian & Popa 1996; Rizescu 1998). However, a few studies indicate a tendency for higher stress drops (Oncescu *et al.* 1999; Popa & Radulian 2000). Oncescu *et al.* (1999), analysing local velocity waveforms, showed that the scaling of the corner frequency (or source duration) with seismic moment for moderate Vrancea earthquakes obeys a constant stress drop law.

However, none of these studies made a systematic analysis of the scaling properties of Vrancea earthquakes over the entire magnitude scale from small and moderate to large magnitudes.

The anomalies in scaling properties of the source spectrum may significantly modify the strong-motion parameters as compared with the ‘average’ case, and therefore are extremely important in seismic hazard studies. For a given magnitude and distance, an unusually high stress drop increases acceleration and velocity amplitudes and decreases the duration of shaking; the effect of a low stress drop is the opposite. As a result, the assumed values of stress drop may have a drastic effect on the seismic hazard assessment (e.g. Radulian *et al.* 2000). Thus, it is of paramount importance to establish the specific source-spectral scaling for the Vrancea zone.

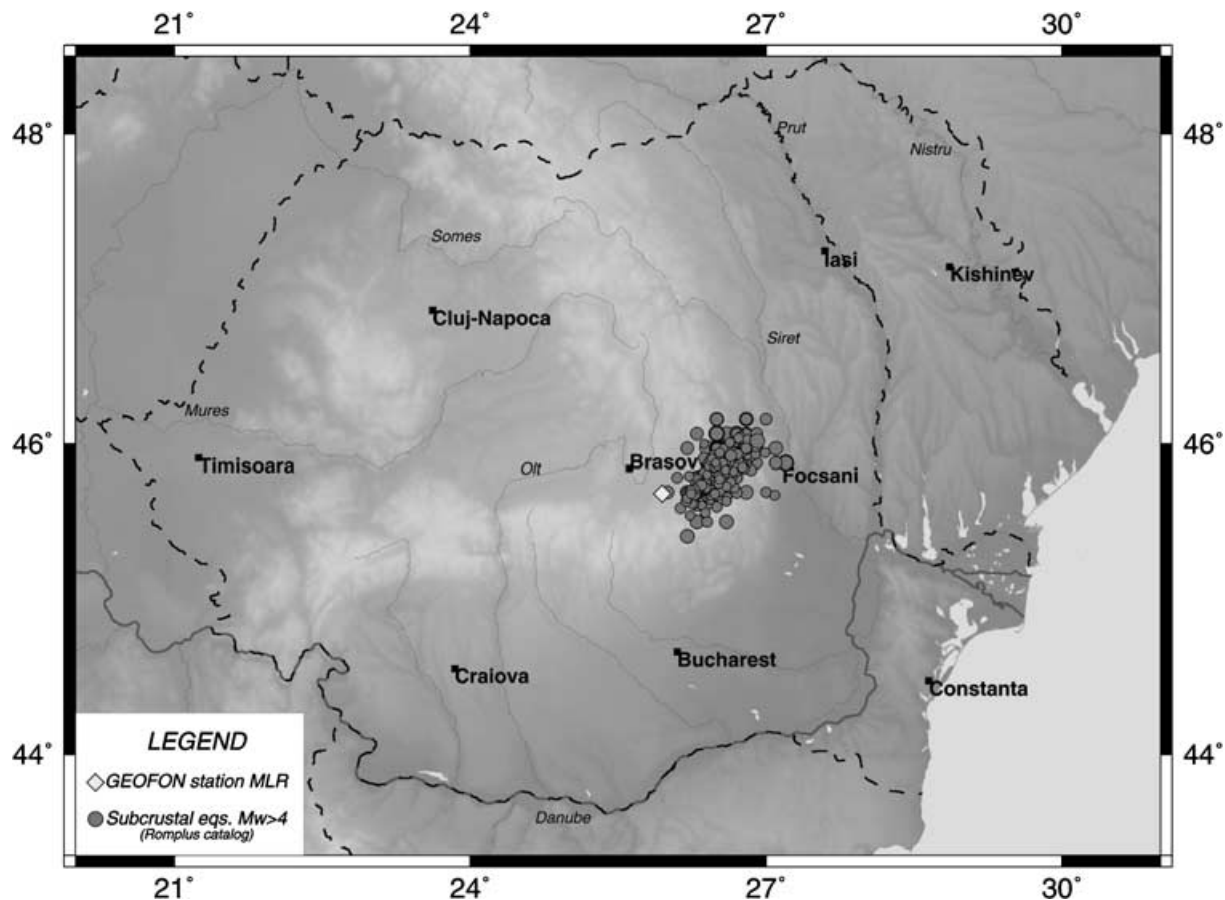


Figure 1. Vrancea seismic zone. Intermediate-depth earthquakes with magnitudes $M_W > 4.0$ from the up-to-date ROMPLUS catalogue are plotted, together with the location of the GEOFON station MLR.

The main goal of this paper is to analyse the scaling properties of the Vrancea intermediate-depth earthquakes and to determine whether the anomalous scaling suggested by the local short-period data is confirmed by the broad-band data recorded at local and global scale. To this end, we analyse a set of 93 broad-band records for 16 moderate and large Vrancea intermediate-depth earthquakes.

OBSERVATIONAL DATA

We consider broad-band waveforms recorded at teleseismic, regional and local distances for 16 intermediate depth Vrancea earthquakes that occurred between 1976 and 2000 ($3.7 \leq M_W \leq 7.4$) (Table 1).

Data from the station GRF (Grafenberg, Germany), affiliated to the German Regional Seismic Network, with a long recording history and located at a relatively small epicentral distance (about 11°) has been pivotal for the success of this study. Data from the GEOFON station MLR (Muntele Rosu, Romania), operated jointly by the GeoForschungsZentrum Potsdam and the National Institute for Earth Physics, Bucharest, located practically in the epicentral zone of Vrancea earthquakes were also highly valuable. Additional data come from representative regional and teleseismic broad-band stations with a reasonable azimuthal coverage for Vrancea earthquakes. We selected stations situated inside continents to minimize storm/surf microseismic noise. The following broad-band stations (situated at epicentral distances given in parentheses) have also been used: TRI (9°), AQU (10°), OBN (11°), ARU (22°), BGCA (41°), HIA (59°), CCM (80°) and ANMO (89°). The waveforms were retrieved via the Internet through the IRIS Data Management Center in Seattle, USA and the GEOFON Data Center in Potsdam, Germany.

ESTIMATION OF SOURCE PARAMETERS

For the events listed in Table 1, all usable P - and S -wave records were processed to estimate the source parameters, in both the frequency and time domain.

The observed velocity data were corrected for instrument response and converted to displacement time-series. The waveforms are plotted together with the theoretical phases and arrival times, based on the traveltimes calculated for the IASP91 Earth model using the Tau software (Buland & Chapman 1983).

Table 1. Selected intermediate-depth Vrancea earthquakes. Locations and magnitudes are taken from the Romanian Earthquake Catalogue ROMPLUS (Oncescu *et al.* 1999), where M_w values are moment magnitudes from teleseismic observations for $M_w > 6.0$ and moment magnitudes, or duration magnitudes from short-period recordings converted to the moment magnitude scale for $M_w < 6.0$. M_W -HARVARD are moment magnitudes as given by the Harvard CMT catalogue on the web site of Harvard University.

Date and origin time	Latitude (deg. N)	Longitude (deg. E)	Depth (km)	M_w	M_W -Harvard
1976/10/01 17:50:43.2	45.68	26.49	146	6.0	
1977/03/04 19:21:54.1	45.77	26.76	94	7.4	7.5
1979/05/31 07:20:06.3	45.55	26.33	120	5.3	5.2
1979/09/11 15:36:54.2	45.56	26.30	154	5.3	5.1
1981/07/18 00:02:58.6	45.69	26.42	166	5.5	
1985/08/01 14:35:04.3	45.73	26.62	93	5.8	5.2
1986/08/30 21:28:35.7	45.52	26.49	131	7.1	7.2
1990/05/30 10:40:06.4	45.83	26.89	91	6.9	6.9
1990/05/31 00:17:47.9	45.85	26.91	87	6.4	6.3
1995/09/06 10:58:45.9	45.53	26.39	120	4.1	
1995/09/19 19:32:21.4	45.63	26.58	143	4.1	
1997/11/18 11:23:16.3	45.78	26.72	126	4.6	
1998/03/13 13:14:37.2	45.51	26.33	165	4.7	5.2
1999/04/04 01:21:12.6	45.70	26.44	146	3.7	
1999/04/28 08:47:56.9	45.47	26.32	145	5.3	5.4
2000/04/06 00:10:39.9	45.69	26.68	136	5.0	5.1

The records of body waves were corrected for attenuation and geometrical spreading. Attenuation affects both the shape and the spectral properties of the P - and S -wave pulses, therefore, to correct for attenuation, we consider the attenuation operator with amplitude spectrum $\exp(-\pi f t^*)$, where f is the frequency and t^* is the travelttime, divided by the quality factor. For the P wave, we assume that t^* is in the range 0.6–1.0 s for teleseismic distances ($\Delta > 20^\circ$), and that it is 0.3 and 0.05 s for regional ($\Delta \sim 10^\circ$) and local distances ($\Delta \sim 0.5^\circ$), respectively. For the S wave, the assumed t^* value is between 2.4 and 4.0 s for teleseismic distances, and is 0.6 and 1.0 s for regional and local distances, respectively. The correction for attenuation is performed in the frequency domain. To calculate the corresponding phase correction that follows from the requirement of causality, a program module from Claerbout (1976) was used. The geometrical spreading coefficients, as given by the relation (Aki & Richards 1980)

$$G(\xi, \mathbf{x}) = \frac{|\mathbf{x}||\xi|}{v(\xi)} \left[\frac{\cos i_x \cos i_\xi \sin \Delta}{p} \left| \frac{\partial \Delta}{\partial p} \right| \right]^{1/2}, \quad (1)$$

(where \mathbf{x} and ξ are the position vectors of the station and focus, respectively, $v(\xi)$ is the seismic wave velocity at the focus, i_x and i_ξ are the incidence angle and take-off angle, respectively, Δ is the epicentral distance and p is the ray parameter) were calculated using the SPHERAY software (available on the Internet at <http://geoscope.ipgp.jussieu.fr>) for an isotropic spherical earth model.

The common ' $\omega^{-\gamma}$ ' spectral model (Brune 1970; Hanks & Wyss 1972), which yields the low-frequency spectral level, corner frequency f_c and high-frequency spectral decay γ , was used to characterize the spectral shape. To determine these parameters from the data, an interactive procedure was programmed using the MATLAB software package. The sequence of operations was performed as follows: for each body-wave pulse, the signal and noise time windows were selected interactively. The noise window was selected before the P onset and was used for both P and S waves. Then, a 5 per cent cosine taper was applied and the displacement spectrum computed using a fast Fourier transform (FFT) algorithm. The signal was noise-corrected by subtracting the estimated noise contribution from the squared spectrum. The spectrum of the signal was inverse-filtered with the attenuation operator, corrected for the geometrical spreading factor and scaled to the seismic moment units. The zero-frequency level, the corner frequency and the slope of the high-frequency decay were determined interactively after visual inspection of the corrected spectrum. The first spectral parameter is an estimate of the seismic moment M_0 and is linked to the moment magnitude by the formulae (Kanamori 1977)

$$M_W = \frac{2}{3}(\log M_0 - 9.1). \quad (2)$$

The interactive mode allowed us to process records with low signal-to-noise ratio, including those with a 0.2–0.3 Hz microseismic spectral peak in the middle of the frequency band analysed. A few examples of the analysed waveforms with high and low signal-to-noise ratios are given in Fig. 2. Signal and noise spectra are also plotted.

The spectral shape was estimated for all usable components and separately for P , pP , sP , S and sS phases, whenever they could be unequivocally identified. Our tests show that the spectra obtained when considering isolated single wave pulses or wave groups (containing P , pP and sP , for example) are consistent with each other, with respect to both corner frequency and spectral slope. The values obtained from the different components of motion also show good consistency. Therefore, the seismic moment, corner frequency and spectral slope for P and S waves have been estimated as averages of all the reliable values determined from the different phases and components of motion (Table 2).

Pulse duration was estimated interactively in the time domain, after low-pass filtering with a cut-off frequency of 2–4 Hz (typical for the teleseismic case) using a fourth-order Butterworth filter to remove the high-frequency noise produced by the normalization with the

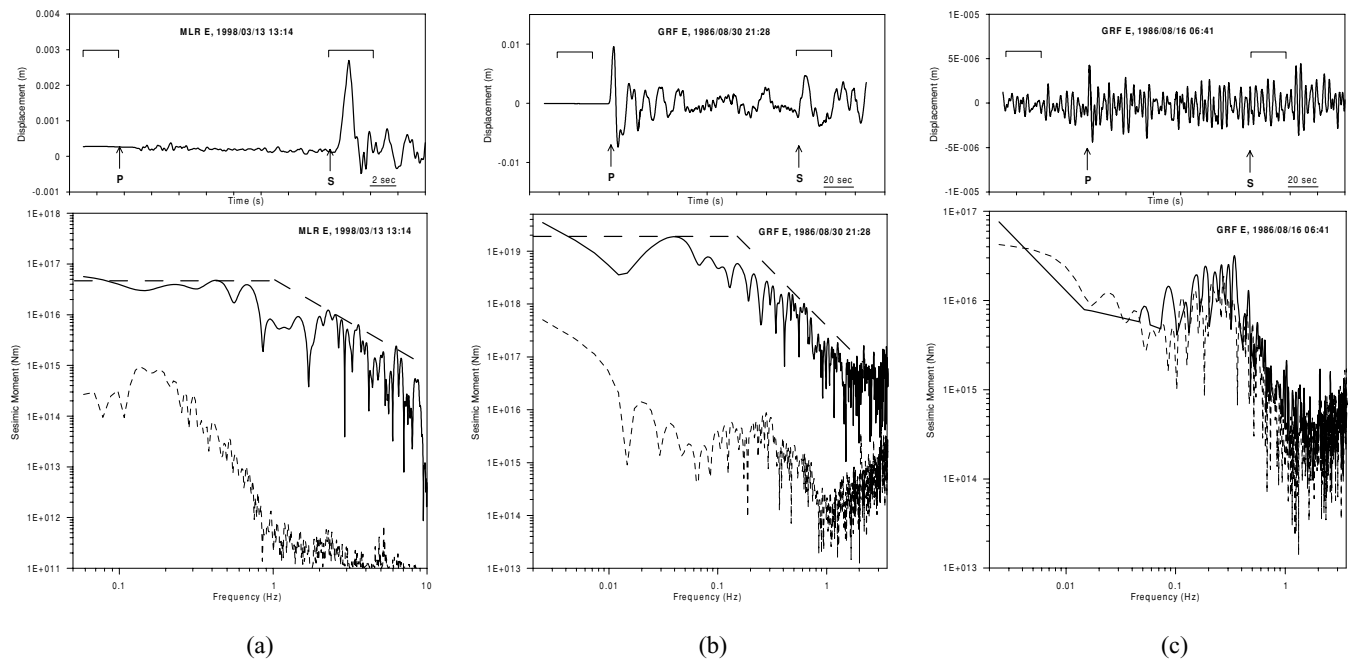


Figure 2. Examples of the waveforms and spectra of Vrancea intermediate-depth earthquakes considered. The signal (*S* wave) and noise spectra are plotted together with the chosen spectral model. The time windows used for spectra computation are indicated by brackets on the time-series plots. Example (a) represents a moderate earthquake ($M_W = 4.7$) recorded at the local station MLR; example (b) represents the strong 1986 event ($M_W = 7.1$) as recorded by the Grafenberg station, at regional distance; example (c) represents a moderate earthquake ($M_W = 4.7$), which could not be used in this study because of the low signal-to-noise ratio, as recorded at the Grafenberg station.

attenuation operator. For the time-domain analysis, only isolated *P* and *S* phases have been considered, and the corresponding results are given in Table 2.

It is interesting to compare our results with previously published estimates of corner frequencies and source durations for Vrancea intermediate depth earthquakes. For larger events, Fuchs *et al.* (1979) estimated from the broad-band recordings of the 1977 event that the f_c for *S* waves was 0.07 Hz, in agreement with our results. Estimates of the width of the source time function for the 1986 event determined from teleseismic recordings (4–6 s by Deschamps *et al.* 1986; 4–10 s by Monfret *et al.* 1990; 7 s by Tavera 1991) match our results well. The source duration derived by Oncescu (1989) for that event from strong ground motion data (4 s) is relatively small compared with ours. This result can be explained by the fact that only an asperity area, and not the whole source area, is ‘seen’ through the spectral window provided by an analogue accelerogram record. Tavera (1991) computed the source durations for the two shocks of 1990 May 30 and 31, inverting long-period *P* waves. His results (5 and 3 s, respectively) agree with our determinations. As for small to moderate Vrancea events, determination of the source parameters using local data (Oncescu 1986; Rizescu 1998; Radulian & Popa 1996), yields values of f_c similar to those that we obtained from the data of station MLR.

We also compared the M_0 and M_W values that we determined from the zero-frequency spectral levels with the corresponding values given by the Romanian earthquake catalogue (Fig. 3). Generally, agreement is quite acceptable, with no systematic bias. In our further analysis we prefer to use the moment magnitude (M_W) values from the regional catalogue, since we consider these estimates, based on all available data for each event, more reliable than our spectral estimates, based, in many cases, on data from a single station.

SCALING RELATIONSHIPS

We now seek to establish the relationship between f_c and M_W that defines the source scaling. The observed $M_W - f_c$ relation is presented in Fig. 4 (for *P* waves) and Fig. 5 (for *S* waves). Linear trends are also plotted that represent the characteristic constant-stress-drop average behaviour, following Brune (1970).

For *S* waves:

$$\log f_{cS} = -0.5 M_W + C_S, \quad (3)$$

where $C_S = 2.25$ or 2.6 for a 1 or 10 MPa stress drop, respectively. This relationship was first established by Thatcher & Hanks (1973) as the average empirical trend for moderate-to-large shallow California earthquakes.

Since these papers, significant progress has been made following Brune’s spectral approach, and for practically all sets of moderate or moderate-to-large shallow earthquakes studied, eq. (3) holds at least approximately. However, values of average stress drop vary significantly,

Table 2. The source parameters (corner frequency, high-frequency spectral slope, pulse duration and moment magnitude) from *P* and *S* waves recorded at the stations listed in the last column. The standard deviation and the number of observations (in parentheses) are also given, when two or more determinations are available.

Event date and time	f_{cP} (Hz)	f_{cS} (Hz)	γ_P	γ_S	τ_P (s)	τ_S (s)	M_{WP}	M_{WS}	Recording station
1976/10/01 17:50	0.35	0.26	1.97	1.42	2.8		4.7	4.8	GRF
	± 0.10 (3)	± 0.06 (3)	± 0.1 (3)	± 0.22 (3)	± 0.8 (2)		± 0.2 (3)	± 0.1 (3)	
1977/03/04 19:21	0.16	0.1	2.73	1.80	10.1	12.9	7.0	6.9	GRF
	± 0.06 (3)	± 0.02 (3)	± 0.15 (3)	± 0.15 (3)	± 1.1 (3)	± 3.7 (2)	± 0.2 (3)	± 0.1 (3)	
1979/05/31 07:20		0.26		1.78		3.5		5.0	GRF
		± 0.04 (2)		± 0.11 (2)				± 0.1 (2)	
1979/09/11 15:36		0.32		1.90		3.4		4.8	GRF
		± 0.03 (2)		± 0.08 (2)		± 0.8 (2)		± 0.1 (2)	
1981/07/18 00:02	0.30	0.28	2.40	1.72	2.6	3.5	5.1	4.9	GRF
	± 0.01 (2)	± 0.01 (2)	± 0.26 (2)	± 0.24 (2)	± 0.0 (2)	± 2.1 (2)	± 0.0 (2)	± 0.1 (2)	
1985/08/01 14:35	0.4	0.33	1.87	1.84	2.0	5.9	4.8	5.0	GRF
	± 0.06 (2)		± 0.58 (2)		± 0.1 (2)		± 0.1 (2)		
1986/08/30 21:28	0.2	0.13	3.25	2.02	4.4	9.2	7.1	6.8	GRF
	± 0.06 (3)	± 0.02 (3)	± 0.32 (3)	± 0.10 (3)	± 0.2 (3)	± 1.1 (3)	± 0.2 (3)	± 0.1	
1990/05/30 10:40	0.19	0.11	2.11	1.94	5.1	9.2	6.7	6.7	AQU, GRF, ARU,
	± 0.11 (30)	± 0.05 (19)	± 0.45 (30)	± 0.22 (19)	± 2.6 (18)	± 2.6 (10)	± 0.2 (27)	± 0.2 (13)	HIA, CCM, ANMO
1990/05/31 00:17	0.30	0.14	2.05	1.98	4.1	8.7	6.0	5.9	AQU, GRF, ARU,
	± 0.13 (21)	± 0.07 (16)	± 0.43 (21)	± 0.46 (16)	± 1.4 (13)	± 4.5 (13)	± 0.2 (16)	± 0.1 (6)	HIA, CCM, ANMO
1995/09/06 10:58		2.43		2.13	0.6	0.5		4.6	MLR
		± 0.04 (2)		± 0.14 (2)		± 0.1 (2)		± 0.1 (2)	
1995/09/19 19:32	3.66	2.33	1.98	1.87	0.3	0.5	3.8	4.0	MLR
		± 0.04 (2)		± 0.06 (2)		± 0.0 (2)		± 0.0 (2)	
1997/11/18 11:23	1.55	1.36	1.57	1.92	1.0	0.6	4.7	5.0	MLR
		± 0.28 (2)		± 0.12 (2)		± 0.2 (2)		± 0.1 (2)	
1998/03/13 13:14	1.67	1.18	2.11	1.93	0.7	1.1	4.8	5.0	MLR
		± 0.06 (2)		± 0.1 (2)		± 0.2 (2)		± 0.1 (2)	
1999/04/04 01:21	4.03	2.9	1.89	1.72	0.3	0.4	4.0	3.7	MLR
		± 0.42 (2)		± 0.08 (2)		± 0.1 (2)		± 0.1 (2)	
1999/04/28 08:47	0.52	0.57	2.21	2.0	2.0	3.9	5.2	5.1	MLR, TRI, GRF,
	± 0.27 (8)	± 0.51 (6)	± 0.26 (8)	± 0.17 (6)	± 0.7 (5)	± 2.7 (6)	± 0.3 (8)	± 0.2 (6)	OBN, ARU, BGCA
2000/04/06 00:10	0.84	1.08	2.54	2.16	1.8	2.9	5.1	5.1	MLR, TRI, GRF,
	± 0.52 (7)	± 0.92 (4)	± 0.44 (7)	± 0.30 (4)	± 0.9 (6)	± 1.9 (6)	± 0.2 (7)	± 0.2 (4)	ARU

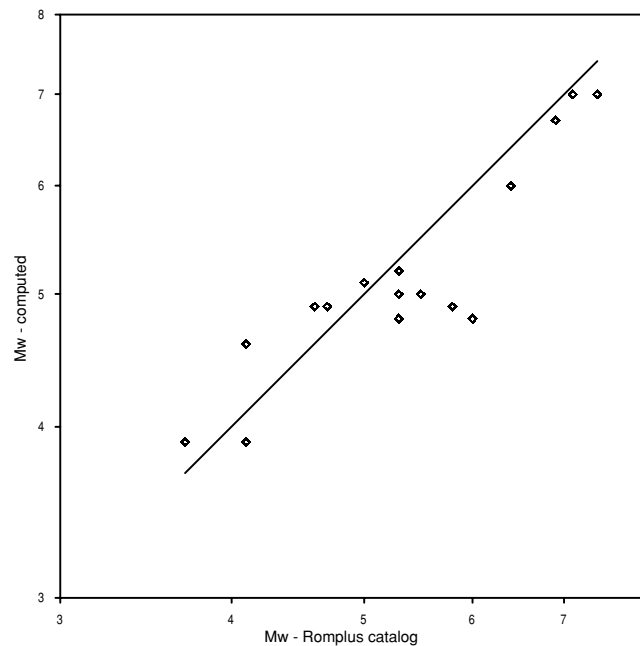


Figure 3. Moment magnitudes determined in this study versus moment magnitudes of the ROMPLUS catalogue. The bisecting line indicates coincidence of both estimates.

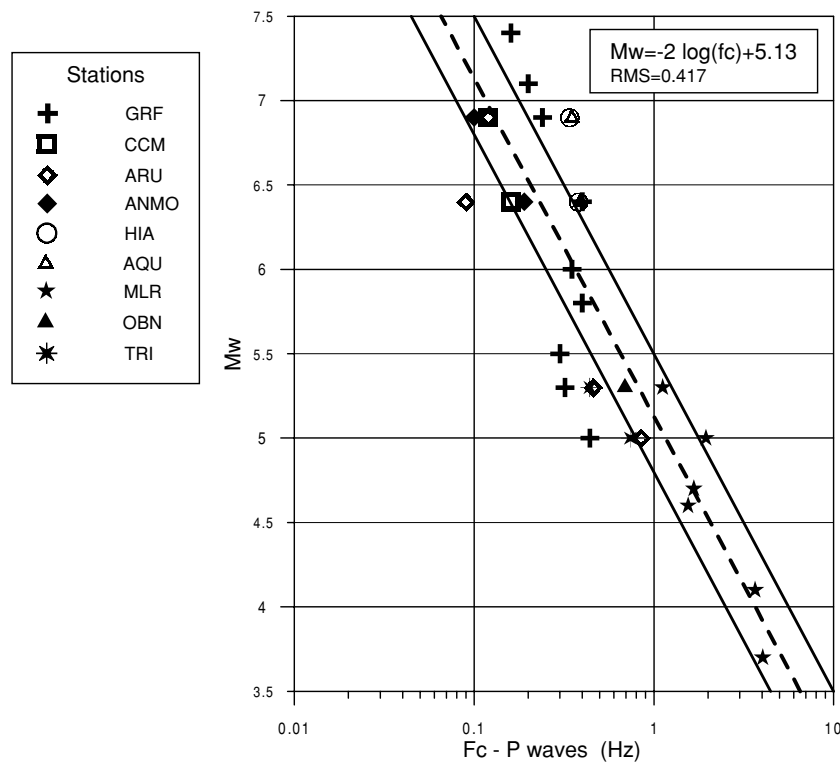


Figure 4. M_W (from the ROMPLUS catalogue) versus P -wave corner frequency for Vrancea intermediate-depth earthquakes. The dashed line represents the data best fit, and is defined by the equation given in the upper right-hand corner. The rms residual of the fit (denoted as ‘rms’) is also given. The solid lines represent the approximate average trends for shallow California earthquakes for a 1 and 10 MPa stress drop.

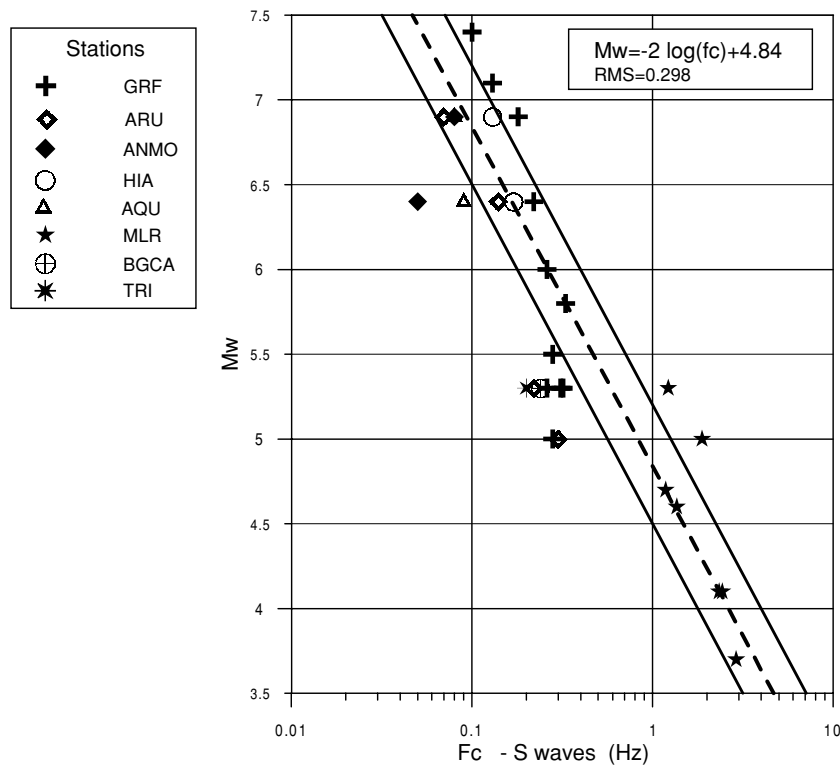


Figure 5. M_W (from the ROMPLUS catalogue) versus the S -wave corner frequency for Vrancea intermediate-depth earthquakes. The dashed line is the best fit to the data, and is defined by the equation given in the upper right-hand corner. The rms residual of the fit (denoted as ‘rms’) is also given. The solid lines represent the approximate average trends for shallow California earthquakes for 1 and 10 MPa stress drop.

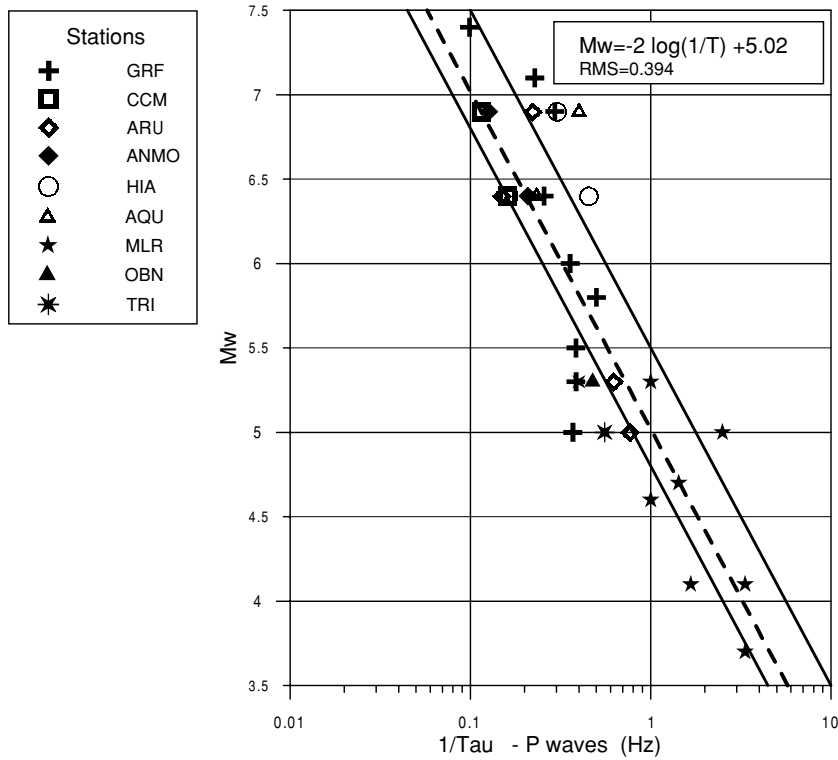


Figure 6. M_W (from the ROMPLUS catalogue) versus the inverse of the P -wave pulse duration for Vrancea intermediate-depth earthquakes. The dashed line is the best fit to the data, and is defined by the equation given in the upper right-hand corner. The rms residual of the fit (denoted as ‘rms’) is also given. The solid lines represent the approximate average trends for shallow California earthquakes for 1 and 10 MPa stress drop.

covering the range 0.5–10 MPa. Part of this scatter reflects differences in processing and analysis procedures and part reflects natural variation between different data sets. To derive the analogue of eq. (3) for P waves, we assume the typical empirical value for the corner frequency ratio:

$$f_{cP}/f_{cS} = 1.4, \tag{4}$$

and obtain

$$\log f_{cP} = -0.5 M_W + C_P, \tag{5}$$

where $C_P = 2.4$ or 2.75 for a 1 or 10 MPa stress drop, respectively. The coefficient 0.5 in eqs (3) and (5) expresses the standard, constant-stress-drop source scaling.

Assuming this scaling, we approximate our data points with a linear relationship with a fixed slope value of -0.5 , and an intercept value obtained from the best fit (dashed lines in Figs 4 and 5). The corresponding values of the stress drops for P and S waves are 3.1 and 3.2 MPa, respectively. These values of stress drop are within the range usually observed for shallow earthquakes when Brune’s approach is used. They are also close to the characteristic values for interplate earthquakes (Kanamori & Anderson 1975). Though this result is evidently a good first approximation, some deviations are seen at the upper-magnitude end, and will be discussed later. Another salient feature of our data set is the unusually high dispersion of the estimates in the magnitude range from 5 to 5.5.

The time-domain estimates behave in a similar way. The $1/T$ versus M_W relationships, plotted in Figs 6 (P wave) and 7 (S wave), are very close to the f_c versus M_W relationships of Figs 4 and 5. This consistency is also visible in the correlation between f_c and source duration (Figs 8 and 9). f_c and the inverse of the source duration closely follow the line with slope 1, only slightly shifted towards smaller $1/T$ values. On average, $f_{cP}/(1/T_P) = 1.0$ and $f_{cS}/(1/T_S) = 1.1$.

Thus, to a first approximation the scaling of Vrancea intermediate depth earthquakes follows the general trend of shallow earthquakes. The ratio of the corner frequency values derived from P and S waves is close, on average, to 1.4, a typical value for shallow earthquakes. The relationship between the inverse pulse durations for P and S waves is similar. The variation in the values obtained from analysis in the frequency domain and in the time domain is comparable for P and S waves (Figs 4, 6 and 5, 7, respectively). The good match between the results of frequency- and time-domain analyses adds additional weight to our general conclusions.

When viewed over the entire range of earthquake size ($M_W = 3.7$ – 7.4), the observed f_c versus M_W trend generally agrees with the constant-stress-drop model (independent of magnitude). However, at the larger-magnitude end, this description seems to fail.

The largest events ($M_W > 6.5$) show a clear tendency for stress drops that are larger than those for moderate-magnitude ones (or, for typical shallow events). From a visual inspection of Figs 4 and 5, one might expect, for $M_W > 7$, stress drop values as high as 10–20 MPa. This possibility is very important for the prediction of future strong motion, because at a given M_W , an increasing stress drop produces a

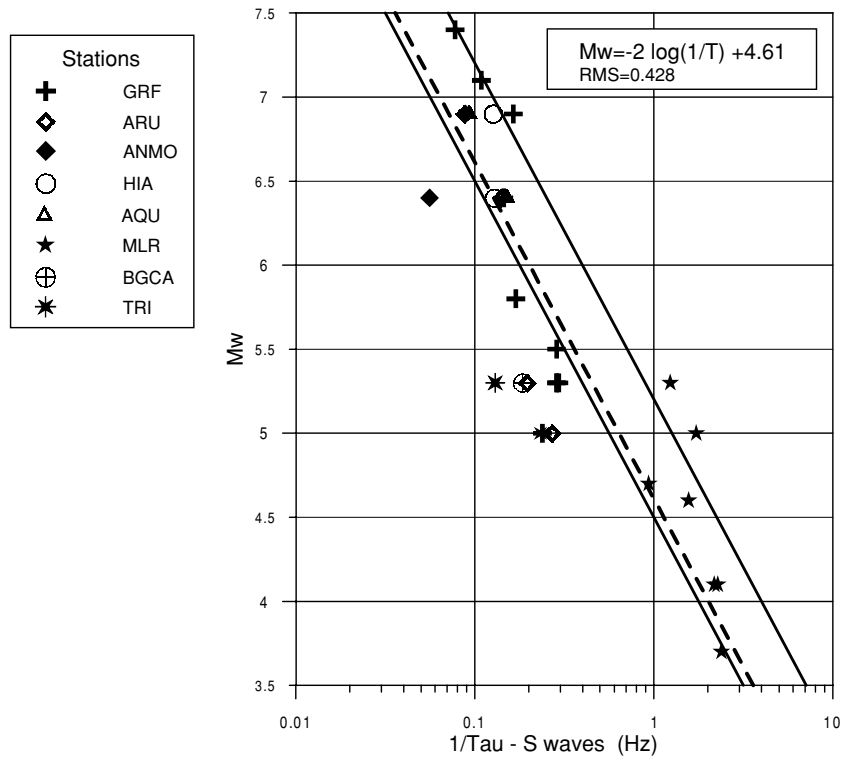


Figure 7. M_W (from the ROMPLUS catalogue) versus the inverse of the S -wave pulse duration for Vrancea intermediate-depth earthquakes. The dashed line is the best fit to the data, and is defined by the equation given in the upper right-hand corner. The rms residual of the fit (denoted as ‘rms’) is also given. The solid lines represent the approximate average trends for shallow California earthquakes for 1 and 10 MPa stress drop.

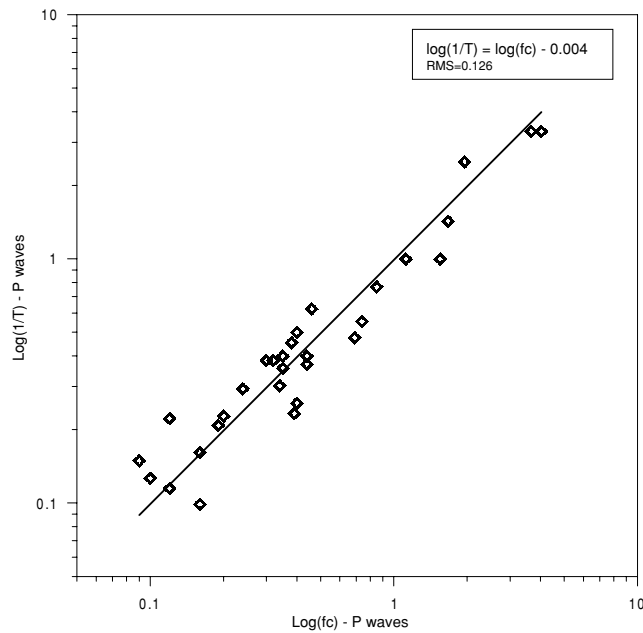


Figure 8. Inverse of the pulse duration versus f_c for the P wave of Vrancea intermediate-depth earthquakes. The best-fitting line, defined by the equation given in the upper right-hand corner, is plotted.

larger peak velocity, acceleration values, response spectra and shorter durations. This conclusion, although based on two cases relying on the data of a single station (GRF), is well supported by independent studies of these same events.

The problem of the existence of a simple and theoretically plausible scaling law is a general one. Theoretical source models usually assume a constant stress drop and constant rupture velocity, resulting in a simple f_c versus M_W scaling, such as that described by eqs (3) and (5). However, natural earthquakes do not necessarily follow such simple assumptions. For example, for Mexican earthquakes (Singh *et al.* 1989) found that when strong-motion amplitudes are extrapolated from moderate to large earthquakes according to the constant-stress-drop

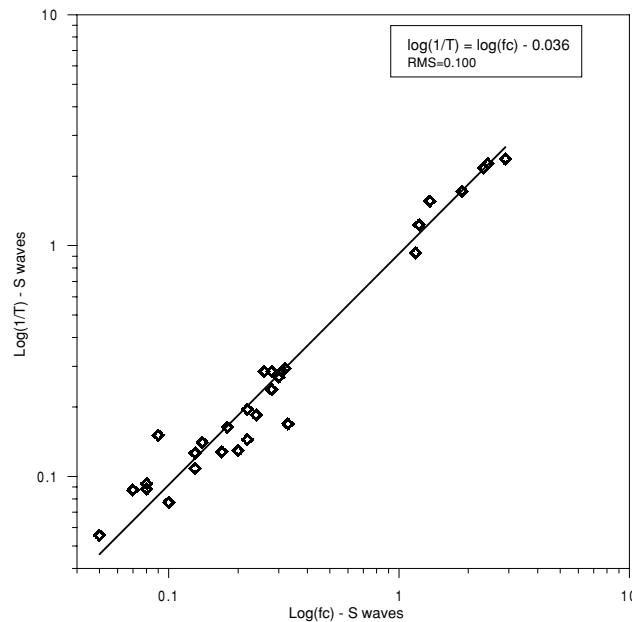


Figure 9. Inverse of the pulse duration versus f_c for the S wave of Vrancea intermediate-depth earthquakes. The best-fitting line, defined by the equation given in the upper right-hand corner, is plotted.

model, the resulting estimates are in excess of those actually observed. The situation in the case of the Romanian earthquakes seems to be the opposite: extrapolation from moderate earthquakes would *underestimate* the strong-motion amplitudes of the largest events somewhat. In such a situation, using empirical rather than ‘theoretically based’ scaling for strong-motion estimates will probably lead to more reliable results. One such case is the study of Moldoveanu & Panza (1999) who, using a kind of empirical source scaling, successfully modelled the main characteristics of the accelerogram recorded in Bucharest from the strong 1990 earthquake ($M_W = 6.9$).

Reviewing the observed data we find some peculiarities. In some cases, the S waveform at the GRF station is one-sided, whereas the P waveform of the same event is of a comparable duration but two-sided (approximately doubling the value of f_c), as seen in the example in the Fig. 2(b). This fact might be explained by a difference between the propagation mode of P and S waves, $\sim 11^\circ$ along this particular path, with a single branch for the S wave and multiple branches for the P wave. These hypothetical path effects might also be responsible for the previously mentioned large data variation in the 5.0–5.5 mag interval. This variation is mainly caused by anomalously low f_c and $1/T$ values obtained only at Grafenberg station. This station is the only one that provides observations for a wide magnitude range, including the largest magnitudes, and thus its use for our study is crucial. For this reason, we decided to consider the GRF data, although they may be contaminated, at least in part, by path effects.

One can ask why we ascribe the observed spectral anomalies in the range $M = 5$ –5.5, with seemingly excessively low corner frequencies, to path effects and yet do not ascribe the anomalies at $M > 6.5$ to path effects in a similar way. Instead we explain the latter as a source effect. The answer is that these two groups of anomalies are of different sign. Almost any path effect broadens the pulse (attenuation, forward scattering, multiple branches). We have been unable to identify a mechanism that *shortens* the pulse, and specifically in the case when we see a unipolar pulse, as we do. For one out of the three events with $M > 7$, we have data from four stations in addition to GRF and they generally support the anomalous behaviour observed at GRF. Indeed, it can be seen that for the most reliable P -wave pulses, logarithmic mean stress drop is above 10 MPa both for frequency- and time-domain processing.

The distributions of the estimated P - and S -wave spectral slopes as functions of magnitude are plotted in Figs 10 and 11, respectively. The γ values for S waves are in the range 1.8–2.0, while the γ values for P waves are generally larger, with a tendency to increase with increasing earthquake size. This tendency, not clearly defined, does not appear to be an artefact of the approximations in our procedure, and deserves some discussion.

The numerical values of our γ estimates are in fact open to question because: (1) true t^* values for the actual paths are unknown and (2) we assume that t^* is frequency-independent and this assumption is probably too simple. The first factor is magnitude-independent and cannot account for the dependence of γ on magnitude, whereas the second factor might provide an explanation. Indeed, our analysis suggests that the true teleseismic t^* may decrease significantly between 1 and 6 Hz, reaching values as low as 0.1–0.2 s at 5–6 Hz. In that case, our correction for attenuation is biased and our γ estimates are based on somewhat biased, excessively gradually sloping spectra. The magnitude of this bias depends on the actual frequency band in which the data are analysed and that, in turn, depends on the signal-to-noise ratio. For the largest magnitudes, the usable frequency band is the widest, so the bias is the largest as well, leading to an underestimate of γ . Therefore, if we ignore the frequency dependence of t^* , we introduce an artificial *decrease* of the γ estimates with increasing magnitude. The actual tendency is the opposite. This may indicate that the increase with increasing magnitude of the value of γ for the P -wave spectra is a genuine phenomenon.

questioned by some indication that the spectral slope increases with increasing magnitude. Unfortunately, these very important results should be considered as just preliminary because of the limited volume of the available data set.

ACKNOWLEDGMENTS

This research is a contribution to the NATO Science for Peace project 972266 ‘Impact of Vrancea Earthquakes on the Security of Bucharest and other Adjacent Urban Areas (Ground Motion Modelling and Intermediate-Term Prediction)’ and to the UNESCO-IUGS-IGCP project 414 ‘Realistic Modelling of Seismic Input for Megacities and Large Urban Areas’.

REFERENCES

- Aki, K. & Richards, P.G., 1980. *Quantitative Seismology*. Vol. 2, Freeman, San Francisco.
- Brune, J.N., 1970. Tectonic stress and the spectra of seismic shear waves from earthquakes, *J. geophys. Res.*, **75**, 4997–5009.
- Buland, R. & Chapman, C.H., 1983. The computation of seismic travel times, *Bull. seism. Soc. Am.*, **73**, 1271–1302.
- Claerbout, J.F., 1976. *Fundamentals of Geophysical Data Processing*, McGraw-Hill, New York.
- Deschamps, A., Monfret, T. & Romanowicz, B., 1986. Preliminary source parameters of the Romanian earthquake of August 30, 1986 from Geoscope network data VLP and BRB channels, *EOS, Trans. Am. geophys. Un.*, **67**, 44.
- Enescu, D., Crisan, E. & Plavita, R., 1979. Determination of the geometric and dynamic focal parameters for some strong intermediate earthquakes in the Vrancea region, *Rev. Roum. Géol., Géophys., Géogr., ser. Géophys.*, **23**, 39–49.
- Fuchs, K. *et al.*, 1979. The Romanian earthquake of March 4, 1977 II. Aftershocks and migration of seismic activity, *Tectonophysics*, **53**, 225–247.
- Hanks, T.C. & Wyss, M., 1972. The use of body-wave spectra in the determination of seismic-source parameters, *Bull. seism. Soc. Am.*, **62**, 561–589.
- Kanamori, H., 1977. The energy release in great earthquakes, *J. geophys. Res.*, **82**, 2981–2987.
- Kanamori, H. & Anderson, D.L., 1975. Theoretical basis of some empirical relations in seismology, *Bull. seism. Soc. Am.*, **65**, 1073–1095.
- Moldoveanu, C.L. & Panza, G.F., 1999. Modelling, for microzonation purposes, of the seismic ground motion in Bucharest due to the Vrancea earthquake of May 30, *Vrancea Earthquakes: Tectonics, Hazard and Risk Mitigation*, pp. 85–98, eds Wenzel, F., Lungu, D. & Novak, O., Kluwer, Dordrecht.
- Monfret, T., Deschamps, A. & Romanowicz, B., 1990. The Romanian earthquake of August 30, 1986: A study based on GEOSCOPE very long-period and broadband data, *Pure appl. Geophys.*, **133**, 367–379.
- Oncescu, M.C., 1986. Some source and medium properties of the Vrancea seismic region, Romania, *Tectonophysics*, **126**, 245–258.
- Oncescu, M.C., 1989. Investigation of a high stress drop earthquake on August 30, 1986 in the Vrancea region, *Tectonophysics*, **163**, 35–43.
- Oncescu, M.C., Marza, V.I., Rizescu, M. & Popa, M., 1999. The Romanian earthquake catalogue between 1984–1997, *Vrancea Earthquakes: Tectonics, Hazard and Risk Mitigation*, pp. 43–47, eds Wenzel, F., Lungu, D. & Novak, O., Kluwer, Dordrecht.
- Popa, M. & Radulian, M., 2000. Test of the empirical Green’s function deconvolution on Vrancea (Romania) subcrustal earthquakes, *Studia Geoph. Geod.*, **44**, 403–429.
- Radulian, M. & Popa, M., 1996. Scaling of the source parameters for the Vrancea intermediate depth earthquakes, *Tectonophysics*, **261**, 67–81.
- Radulian, M., Vaccari, F., Măndrescu, N., Panza, G.F. & Moldoveanu, C.L., 2000. Seismic hazard of Romania: deterministic approach, *Pure appl. Geophys.*, **157**, 221–247.
- Räkers, E. & Müller, G., 1987. The Romanian earthquake of March 4, 1977, *J. Geophys.*, **50**, 143–150.
- Rizescu, M., 1998. A completely automated system for seismological data acquisition, processing and exchange, *PhD thesis*, Institute for Atomic Physics, Bucharest, p. 219.
- Singh, S.K., Ordaz, M., Anderson, J.G., Rodriguez, M., Quaaas, R., Mena, E., Ottaviani, M. & Almora, D., 1989. Analysis of near source strong-motion recordings along the Mexican subduction zone, *Bull. seism. Soc. Am.*, **79**, 1697–1717.
- Tavera, J., 1991. Étude des mécanismes focaux de gros séismes et sismicité dans la région de Vrancea, Roumanie, *Raport de Stage de Recherche*, Institut de Physique du Globe, Paris, p. 53.
- Thatcher, W. & Hanks, T.C., 1973. Source parameters of Southern California earthquakes, *J. geophys. Res.*, **78**, 8547–8576.
- Trifu, C.-I. & Oncescu, M.C., 1987. Fault geometry of August 30, 1986 Vrancea earthquake, *Ann. Geophys.*, **5**, 727–730.
- Trifu, C.-I., Deschamps, A., Radulian, M. & Lyon-Caen, H., 1992. The Vrancea earthquake of May 30, 1990: an estimate of the source parameters, *Proc. 22nd ESC Gen. Ass.*, Barcelona, 1990, Vol. 1, pp. 449–454.